HHS Public Access

Author manuscript

J Am Soc Mass Spectrom. Author manuscript; available in PMC 2022 May 05.

Published in final edited form as:

J Am Soc Mass Spectrom. 2021 May 05; 32(5): 1237–1248. doi:10.1021/jasms.1c00072.

Complementary structural information for stressed antibodies from hydrogen-deuterium exchange and covalent labeling mass spectrometry

Catherine Y. Tremblay[a], **Patanachai Limpikirati**[b], **Richard W. Vachet**[a,*]

[a]Department of Chemistry, University of Massachusetts, Amherst, Massachusetts 01003, United States [b]Current Address: Department of Food and Pharmaceutical Chemistry, Faculty of Pharmaceutical Sciences, Chulalongkorn University, Bangkok 10330, Thailand

Abstract

Identifying changes in the higher-order structure (HOS) of therapeutic monoclonal antibodies upon storage, stress, or mishandling is important for ensuring efficacy and avoiding adverse effects. Here, we demonstrate diethylpyrocarbonate (DEPC)-based covalent labeling (CL) mass spectrometry (MS) and hydrogen deuterium exchange (HDX)/MS can be used together to provide site-specific information about subtle conformational changes that are undetectable by traditional techniques. Using heat-stressed rituximab as a model protein, we demonstrate that CL/MS is more sensitive than HDX/MS to subtle HOS structural changes under low stress conditions (e.g. 45 and 55 °C for 4 h). At higher heat stress (65 °C for 4 h), we find CL/MS and HDX/MS provide complementary information, as CL/MS reports on changes in side chain orientation while HDX/MS reveals changes in backbone dynamics. More interestingly, we demonstrate that the two techniques work synergistically to identify likely aggregation sites in the heat-stressed protein. In particular, the C_{H3} and C_L domains experience decreases in deuterium uptake after heat stress, while only the C_{H3} domain experiences decreases in DEPC labeling extent as well, suggesting the C_{H3} domain is a likely site of aggregation and the C_L domain only undergoes a decrease in backbone dynamics. The combination of DEPC-CL/MS and HDX/MS provides valuable structural information, and the two techniques should be employed together when investigating the HOS of protein therapeutics.

Graphical Abstract

*To whom correspondence should be addressed: rwvachet@chem.umass.edu.

Disclosure statement

The authors report no conflict of interest.

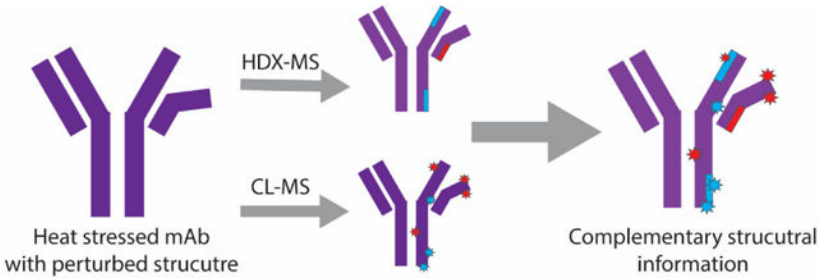

Keywords

Antibody therapeutics; Covalent labeling; Diethylpyrocarbonate; Hydrogen/deuterium exchange; Mass spectrometry; Protein higher-order structure; Rituximab

Introduction

The market for monoclonal antibodies (mAbs) has grown tremendously in the past 25 years and is estimated to be a $300 billion market in 2025. [1-4] As the mAb market is growing, there is an increasing need to characterize their higher order structure (HOS) quickly and effectively. Unlike small molecules, mAb structure is complex, and changes in HOS resulting from mishandling or storage can lead to reduced stability, loss of efficacy, or possible immunogenicity.[5,6] In addition to monitoring changes in HOS, general structural information is useful for biologics license applications as it is necessary to demonstrate lot-to-lot comparability and stability.[7] Methods to assess HOS are also essential in biosimilar development as comparability of a biosimilar to an approved drug is necessary for FDA approval.[8]

Detecting mAb HOS changes is difficult due to their complexity and multidomain nature. High resolution methods such as nuclear magnetic resonance (NMR) or X-ray crystallography can provide atomic-level resolution; however, these techniques require large amounts of sample, have difficulty with heterogeneous proteins (e.g. multiple glycoforms), and/or are incapable of analyzing high molecular weight mAbs. Conversely, low-resolution techniques such as differential scanning calorimetry, dynamic light scattering, fluorescence spectroscopy, infrared spectroscopy, and circular dichroism spectroscopy are relatively fast and have low sample consumption, but they do not provide site-specific information about localized conformational changes. As a result, there is a need for methods that are rapid, low on sample consumption, and provide high enough resolution to detect site-specific HOS changes.

Mass spectrometry (MS) is a powerful tool for protein analysis and has some advantages over other structural characterization techniques. MS-based methods have the benefits of limited sample consumption, essentially no molecular weight limitation, and the ability to analyze complex protein mixtures. MS is emerging as a method that can examine protein HOS.[7,9] To characterize protein HOS, protein structural information must be encoded into the protein's mass. One commonly used method to achieve this is hydrogen deuterium exchange (HDX). HDX/MS is well established in industry for detecting protein dynamics,

protein/protein interactions, and protein-ligand binding, including for mAbs.[10-18] In HDX/MS the exchange of backbone amide hydrogens with deuterium is measured, and the extent of exchange depends on solvent accessibility, H-bonding, and dynamics, resulting in an increase in mass that can be detected and localized to peptide fragments using MS after proteolytic digestion.

Covalent labeling (CL) with MS detection has also been used increasingly to characterize protein HOS such as protein-ligand binding sites and protein/protein interactions,[19,20] and recently the method has been applied for structural analysis and epitope-paratope mapping of antibodies.[19,21-25] In CL a reagent is used to covalently modify solvent exposed amino acid side chains, resulting in a mass shift that can be detected with MS. When used with bottom-up tandem MS (MS/MS), residue-level resolution can be obtained, which contrasts with typical HDX measurements that are limited to peptide-level information. CL/MS methods have the additional advantage of being permanent modifications that are typically not lost during analysis, as can happen to deuterium labels during HDX/MS.

HDX/MS and CL/MS are complementary methods as HDX provides protein backbone information while CL reports on side chains. The complementarity of the two techniques has recently been used to gain deeper structural information about a variety of protein systems.[21,26-28] For example, Gross and coworkers have used fast photochemical oxidation of proteins (FPOP), which is a CL/MS method, and HDX/MS to investigate the conformational changes that take place in the interleukin-6 receptor when it binds with different adnectins. The same group also used FPOP and HDX/MS to structurally characterize antibodies, finding that the two methods provide overlapping results, while FPOP was able to identify potential residues within the epitope.[26] An important aspect of FPOP is the hydroxyl radicals that are used react on the μs to ms timescale, which is similar to the intrinsic (or chemical) exchange rate of HDX. Our group recently demonstrated other CL reagents, such as diethylpyrocarbonate (DEPC), which react on a slower time scale (i.e. s) can be combined with HDX/MS data to provide synergistic structural information about protein-ligand interactions.[29] DEPC reacts with nucleophilic residues, including Cys, Lys, His, Thr, Ser, and Tyr, labeling around 30% of the surface exposed residues on the average protein. HDX/MS measures both changes in solvent exposure and dynamics, which can lead to uncertainty when studying protein interactions, while CL/MS with DEPC is primarily sensitive to changes in solvent exposure because of the relatively slow-reacting nature of the reagent. Moreover, unlike typical HDX experiments that are done at different time points (e.g. 10 s to 24 h), CL experiments are typically conducted at a single reaction time point (e.g. 5 min), and thus lack the kinetic information that might report on dynamics. Together, the two techniques can provide greater insight into binding sites and binding-induced structural or dynamical changes.

Here, we demonstrate HDX/MS and DEPC-based CL/MS can be used to provide complementary and synergistic HOS information about heat-stressed therapeutic mAbs, using rituximab as a model system. Three levels of heat stress were chosen to induce different extents of structural changes to compare the information provided by these two techniques. Under low and moderate heat stress (i.e. 45 °C and 55 °C), the two methods provide complementary information about regions of rituximab that undergo subtle

structural changes. By using high heat stress conditions, just below the melting temperature of the protein, we demonstrate that the two techniques together more clearly differentiate structural changes resulting from changes in protein dynamics from those resulting from decreases in solvent exposure due to aggregation. The techniques provide greater confidence in the aggregation sites by using CL data to clarify ambiguous HDX results. Together, DEPC-based CL/MS and HDX/MS provide a more comprehensive picture of the structural changes that take place in a heat-stressed mAb.

Methods

Materials

Rituximab formulation (Rituxan® 100 mg/10 mL vial, lot# 3209283, Genentech) was purchased from Myoderm. Diethylpyrocarbonate (DEPC) (#D5758), imidazole (#I5513), iodoacetamide (#I6125), tris(2-carboxyethyl)phosphine (TCEP) (#C4706), deuterium oxide (D2O) (#151882), Guanidine hydrochloride (GnHCl) (#G3272), sodium chloride (#S5886), and trypsin (#T1426) were obtained from Sigma-Aldrich. Urea (#AC424581000) was purchased from Acros Organics. Sodium phosphate monobasic monohydrate (#S0710-1) was obtained from EM Science. Sodium phosphate dibasic anhydrous (#S374-500), LC/MS-grade formic acid (#A117-50), acetonitrile (#A998-4), and water (#W7-4) were purchased from Fisher Scientific.

Heat treatment

Formulated rituximab was used in all experiments. The formulation consists of 10 mg/mL (69.5 μM) rituximab, 0.7 mg/mL polysorbate 80, 7.35 mg/mL sodium citrate dihydrate and 9 mg/mL sodium chloride in water at pH 6.5. Samples were aliquoted from a rituximab formulation stored at 4 °C. Control samples were incubated at 37 °C for 5 min, and heat-stressed samples were incubated at 45 °C, 55 °C, and 65 °C for 4 h in a water bath prior to cooling to an appropriate temperature for DEPC labeling or HDX experiments.

DEPC labeling and proteolytic digestion

DEPC stock solutions were prepared in acetonitrile and further diluted in water in order to have acetonitrile levels that are less than 1% v/v in the final samples. The DEPC labeling reaction was done on the rituximab formulation (5 μL aliquot) with only a small dilution (to 58 μM) due to the addition of DEPC. Labeling was conducted at a DEPC:protein molar ratio of 4:1 at 37 °C for 5 min. We have found that a 5-min reaction a 4:1 molar ratio leads to sufficient labeling of antibodies without perturbing the protein's structure.[30] Imidazole was then added at a 1:50 DEPC:imidazole molar ratio to quench the reaction. For each stress conditions, at least three replicates were performed on the rituximab samples.

The quenched reaction mixtures were subsequently added into a urea-containing microtube and diluted in 50 mM phosphate buffer (pH 7.4). Protein denaturation was conducted in an 8 M urea solution. To reduce the disulfide bonds and alkylate the reduced Cys residues, TCEP and iodoacetamide were both added at final concentrations of 25 mM. The samples were kept in the dark for 20 min at room temperature to prevent photodegradation of iodoacetamide. DetergentOUT™ Tween® Micro spin columns (#786–214, G-Biosciences)

were then used to remove polysorbate 80 from the samples. Subsequently, samples were diluted 4-fold with phosphate buffer to ensure less than 2 M urea was present during the digestion. Proteolytic digestion was performed using trypsin at a 1:10 (w/w) enzyme to substrate, and the protein was digested overnight at 37 °C. To remove trypsin and collect the resulting peptides after the digestion, the samples were filtered through an Amicon® centrifugal filter with a 10 kDa molecular weight cutoff (#UFC501096, Millipore). The filtrate was collected, flash-frozen in liquid nitrogen, and stored at −20 °C until LC-MS/MS analysis.

LC-MS/MS of CL samples

For online LC-MS/MS analyses, a sample containing approximately 2 μg of rituximab peptides was loaded on an Easy-NanoLC 1000 system (Thermo Scientific). The flow rate was set at 300 nL/min. An Acclaim PepMap C18 trap column (2 cm × 75 μm, 3 μm, Thermo Scientific) was used for sample trapping and desalting. The separation of peptides was then performed using a FortisBIO C18 nanocolumn (15 cm x 75 μm, 1.7 μm; Fortis Technologies). LC/MS-grade water (solvent A) and acetonitrile (solvent B), each containing 0.1% formic acid, were used as mobile phases. A linear gradient of solvent B was increased from 0% B to 50% B over 90 min. A nanoelectrospray ionization was used as an ion source at a needle voltage of 2100 V (positive mode). Mass spectra were acquired on a Thermo Scientific Orbitrap Fusion mass spectrometer. Tandem mass spectrometry (MS/MS) was conducted using collision-induced dissociation (CID) on a linear quadrupole ion trap.

CL/MS data analysis

Details about a custom software pipeline designed specifically for protein DEPC CL/MS experiments were described previously.[31] Briefly, CID tandem mass spectra were searched against the sequence database to achieve peptide mapping with labeled site identification. The search parameters were set as follows: a precursor mass tolerance of 10 ppm, a product ion tolerance of 0.5 Da, carbamidomethylation of Cys and DEPC modification of His, Lys, Ser, Thr, Tyr, and N-terminus (mass addition of 72.0211 Da) as variable modifications. For semi-quantitation of modification extent, peak areas of labeled and unlabeled species obtained from reconstructed ion chromatograms of each species are used to calculate percent labeling at each labeled site.

HDX procedure

Samples were aliquoted (15 μL) from a rituximab formulation stored at 4 °C and then were incubated at 45 °C, 55 °C, or 65 °C for 4 h in a temperature-controlled water bath. After incubation, samples were diluted to 3 mg/mL and cooled to 10 °C for 15 min prior to HDX. Control samples were diluted to 3 mg/mL, and then cooled to 10 °C for 15 min prior to HDX.

D_2O was prepared in a 10 mM phosphate buffer. The pD was adjusted via a pH meter corrected by the following relationship: pD = pH reading + 0.41.[32] HDX experiments were conducted using the Leap HDX Automation Manager as part of the Waters nanoACQUITY UPLC system (Waters Corporation, Milford, MA, USA). The HDX procedure, including the

exchange reaction, quench, proteolytic digestion, LC separation, and MS conditions are detailed in the SI.

A 3.0 μL aliquot of native or stressed rituximab sample was diluted into 57.0 μL D_2O buffer and allowed to exchange for various lengths of time ranging from 10 s to 24 h at 10 °C. At the end of each exchange period, the reaction was quenched by mixing the sample with a quenching buffer (1:1, v/v) that contained 4 M GnHCl, 0.5 M TCEP, and 200 mM Na_2PO_4 in water (pH = 2.5) at 1 °C for 5 min. After the quench step, the sample was transferred and injected into the Waters ACQUITY UPLC System.

LC-MS of HDX samples

Online digestion was performed using a Waters ENZYMATE immobilized pepsin column (ID: 2.1 length: 30 mm) at high pressure (~11000 psi) and 10 °C. The proteolytic peptides were collected by a trap column (HSS T3 pre-column, 100 Å, 1.8 μm, 2.1 mm X 5 mm, Waters) for 4.5 min at 0 °C. Then, trapped peptides were eluted into a Waters ACQUITY C18 column (2.1 x 50 mm, 1.8 μm). The LC separation was conducted using binary solvent system; solvent A was water with 0.1% formic acid at pH 2.5, and solvent B was acetonitrile with 0.1% formic acid. The separation was carried out at 0 °C with a linear gradient that was increased from 5% B to 35% B over 7 min. The column was then washed by increasing from 35% B to 85% B in 1 min at a flow rate of 40 μL/min. The eluent was then directed into a Waters SYNAPT G2Si mass spectrometer for analysis in MS^E mode over the m/z range of 50-2000.

HDX data analysis

The deuterium uptake level of each measured peptide at different exchange time points was automatically calculated using the Waters DynamX 3.0 software. Each peptide was manually inspected. Sequence coverage is >80% for all conditions. Averaged values from triplicate experiments with propagated error are reported. The reported deuterium uptake values are not corrected for back-exchange. Back exchange experiments were performed as described previously, and back exchange ranged from 30 to 50% for the measured peptides.[33] The relatively long quench times (i.e. 5 min) and high pressure digestion conditions facilitate protein digestion at the expense of higher back exchange. However, back exchange was still within an acceptable range.[33] Differences in exchange at the peptide level comparing native and heat stressed states were calculated in Excel for peptides that had 4 or more time points in at least 2 trials. Peptides were found to be statistically different if they were 3σ outside of the average of all differences for all time points and for all peptides. For the 45 °C samples, the ΔD that indicated significant difference was found to be 0.21 Da. For 55 °C, the value was 0.30 Da, and for 65 °C it was 0.46 Da. Peptides were further validated as significant by calculating their deuterium uptake change on a per residue basis (ΔD / # of exchangeable residues in peptide), with peptides being considered significantly different if they were 3σ outside the average of the per residue change. The peptides that were significantly different by absolute difference in deuterium uptake and per residue difference in deuterium uptake were consistent with each other for 45 °C and 55 °C; however, for the 65 °C data, some peptides that were found to be different by absolute value were not significantly different on a per residue basis. These peptides were still considered different, as no peptide was

significantly different on only a per residue basis. The ion intensities of the peptides that exhibited two different exchange distributions were exported to the program Origin, and multiple peak fitting was used to fit separate Gaussians to each distribution so that the exchange rates could be determined.

Biophysical characterization and activity assays—The technical details of these methods can be found in the Supplementary Material.

Results

Heat stress at 45 °C for 4 h

HDX and DEPC-CL with MS detection were used to identify any HOS changes experienced by rituximab after heat stress. Each heavy chain/light chain dimer of rituximab contains 236 total His, Lys, Tyr, Thr, and Ser residues that can be labeled by DEPC (Table S1). After heating the protein at 45 °C for 4 h and then reacting it with DEPC, we find 154 residues are labeled, but only 17 undergo a significant change in labeling extent in comparison to the unheated (i.e. 37 °C) state (Table 1). These 17 residues are scattered throughout the protein and do not cluster in any one location (Figure 1A). Moreover, 12 of these 17 residues are Ser, Thr, and Tyr, whose CL reactivity with DEPC is influenced by the microenvironment around these residues,[25] suggesting the changes in reactivity are primarily due to the re-orientation of these side chains. The majority of the remaining five Lys and His residues that undergo changes are found to increase in labeling, which is consistent with mild heating leading to minor structural changes in some protein molecules that cause higher solvent exposure of these residues. These minor structural changes, however, do not cause any significant changes in HDX between the 45 °C heated and native states (Figure 1B and S1). Importantly, three of the 87 peptides used for the HDX/MS analysis exhibit two exchange distributions in both the stressed and the native state, indicating that at least two different conformations of rituximab exist in solution (Figure S2). However, these three peptides do not show any significant difference between the 45 °C stressed and native conditions. Additionally, activity and biophysical assays show no significant change in rituximab upon heating at 45 °C for 4 h (Figures S3 and S4). Overall, it appears that the structure of rituximab is not significantly altered after 4 h of heat stress at 45 °C.

Heat stress at 55 °C for 4 h

After heating rituximab at 55 °C for 4 h, changes in DEPC CL (Table S2) are primarily clustered in the F_{ab} region, with scattered CL increases in the F_c region (Figure 2A). Out of the 236 labelable residues, 133 are labeled, while 31 undergo a significant change in labeling extent upon heat stress. Like the 45 °C heat stress condition, the majority (70%) of residues that undergo CL changes are Ser, Thr, and Tyr residues (Table 1). Most of the remaining His and Lys residues that change in labeling undergo increased CL, which one would expect upon heating, as some protein molecules partially unfold and have increased side chain solvent accessibility. The His and Lys residues that have increased CL mostly reside in the F_{ab} and hinge regions. HDX/MS data show that one region of the protein, 148-171, in the C_L domain undergoes increased deuterium uptake (Figure 2B and Figure S5). The differences in deuterium uptake of this peptide disappears after 24 h of exchange. Identical deuterium

exchange after 24 h, while having differential uptake at shorter exchange times (i.e. 1 and 4 h), is consistent with increases in protein dynamics, which likely occur upon protein heating.

Closer inspection of the HDX data reveals that eight out of the 80 peptides are found to have two exchange distributions, again suggesting two conformations in solution. Three of these peptides come from the C-terminal end of the light chain, four come from the C-terminal end of the heavy chain, and one is from the middle of the C_{H1} domain. These two distributions can be separated into “slow exchangers” and “fast exchangers” (Figures S6 and S7), yet we find no significant differences between the slow and fast exchangers for these peptides upon comparing the native and 55 °C stress states. So, even if new protein conformations are populated in these regions upon heating at 55 °C, they are not readily resolvable by HDX/MS. Only the region spanned by 148-171 in the C_L domain undergoes a significant change in exchange. The change in HDX in this one location and the changes in DEPC labeling extent are supported by activity assays that show significant changes in F_{ab} activity. The activity assay results for the F_c region are somewhat ambiguous (Figure S3), and circular dichroism spectroscopy is insensitive to these changes at 55 °C (Figure S4).

Heat stress at 65 °C for 4 h

After heating rituximab at 65 °C for 4 h, significant structural changes are apparent from both DEPC CL/MS (Table S3) and HDX/MS results. Visually, the solution becomes cloudy, which is indicative of protein aggregation, but this cloudiness mostly disappears upon dilution for the labeling experiments. Moreover, dynamic light scattering and size-exclusion chromatography experiments reveal the existence of larger molecules in solution, further confirming aggregation (Figure S8). Because the measured sequence coverage is comparable for the 45 °C, 55 °C, and 65 °C experiments, we do not feel that the observed aggregation has affected our results significantly.

While 65 °C is below the melting temperature of rituximab, the protein was heated at this temperature for 4 h to cause significant structural changes that we expected to be measurable by the two MS techniques.[35] Significant changes in CL extent are observed for 22 residues, and six peptides are found to undergo significant changes in deuterium uptake. Of the 22 residues, seven increase and 15 decrease in CL, while two of the six peptides increase in HDX and four decrease (Figure 3). Notably, one of the two peptides that increases in exchange is the same peptide (i.e. 148-171) that increases in exchange when heated at 55 °C, suggesting this part of the protein is prone to unfolding or increased dynamics after heating (Figure S9).

Additionally, seven of the 128 peptides considered in the HDX analysis have two exchange distributions, indicating multiple conformations (Figures S10, S11, and S12). In two of the seven peptides that display multiple conformations, the slow-exchanging conformation becomes more abundant after heating, which is consistent with these sites becoming buried due to aggregation in a fraction of the protein molecules. Considering the data overall, the results from CL/MS and HDX/MS are generally consistent with each other (Table 2). The relatively few increases in CL and deuterium uptake occur in the F_{ab} region, while decreases are measured throughout the protein (Figure 3A and B). The prevalence of decreased

labeling and exchange is expected due to the protein aggregation that occurs at this temperature.

While the CL/MS and HDX/MS results are mostly consistent, a closer inspection of the 65 °C data provides a useful comparison of the information provided by the two techniques. Residues that undergo changes in DEPC labeling are located within regions that have either (i) no coverage by HDX, (ii) no change in HDX, (iii) the opposite change as HDX, or (iv) the same change as HDX (Table 2). While we have excellent protein sequence coverage (> 80%) in our HDX/MS experiments (Figure S13), two of the 22 residues that undergo changes in CL are in regions lacking coverage by HDX/MS, making it difficult to compare the data for these residues. Fifteen of the residues that undergo CL changes are in regions with no change in deuterium uptake, with five having increased CL and the other 10 undergoing decreased labeling. The CL decreases are mostly for Ser, Thr, or Tyr residues, which are sensitive to changes in the side chain microenvironment. This inherent sensitivity to changes in microenvironment may explain why CL changes are observed and HDX changes are not. The CL reactivity of Ser, Thr, and Tyr residues is exquisitely sensitive to changes in microenvironment, as is seen in the 45 °C data, whereas more substantial structural changes are necessary to result in measurable changes in HDX/MS.[36]

Only one residue, Thr101, undergoes a change in CL that appears to be the opposite of the HDX results. Thr101 undergoes decreased CL and is located in a peptide (94-103) in the heavy chain that increases in deuterium uptake after heating. Two other residues in the protein region spanned by this peptide are also covalently labeled, but their CL changes are statistically insignificant (i.e. Thr96 [2.0 ± 0.6% to 4 ± 2%] and Lys102 [0.08 ± 0.02% to 0.04 ± 0.02%], see Table S3). The CL increase for Thr96 might be consistent with the HDX increase in this protein region, but the poor measurement precision for this residue does not allow us to draw this conclusion with confidence.

Finally, four residues undergo CL changes that are consistent with the HDX results. Ser428, His439, Tyr440, and Lys451 undergo a decrease in CL after heating at 65 °C, and a peptide measured by HDX/MS that spans this region of the heavy chain (428-450) also undergoes a decrease in deuterium uptake. This peptide exhibits both slow and fast-exchanging distributions in the native and heat-stressed states. Interestingly, only the slow-exchanging distribution decreases in exchange in the stressed state, while the fast-exchanging distribution increases in exchange in the stressed state. Furthermore, this 28-residue region of the protein contains nine residues that are covalently labeled (see Table S3). Unlike Ser428, His439, Tyr440, and Lys451, five residues (Ser430, His433, His437, Lys443, and Ser448) do not undergo statistically significant changes in labeling. These observations point to a mixture of conformations and some complex structural changes to this region of the protein.

Discussion

The work described here is one of the first studies that has used CL/MS and HDX/MS together to examine the same heat-stressed mAb. While a few other studies have reported oxidative labeling (e.g. FPOP)[21,37] together with HDX/MS to analyze mAb structure and

interactions, the use of DEPC as the labeling agent in this study provides a unique set of information for stressed mAbs because of the rate at which the reagent reacts with residue side chains. Our results support the idea that DEPC CL/MS can be more sensitive to subtle structural changes than HDX/MS. In addition, we demonstrate that the methods are complementary, as might be expected, but they also provide some synergistic information, yielding new insight not available from either technique alone.

CL is more sensitive than HDX

The CL/MS results for rituximab at 45 and 55 °C indicate that DEPC-CL is more sensitive to subtle HOS changes than HDX. After heating at 45 °C, no significant changes in HDX are detected, while 17 residues undergo changes in CL extent. About 70% of the changes in DEPC-CL are residues that are weakly nucleophilic, namely Ser, Thr, and Tyr. The sensitivity of DEPC CL/MS to subtle structural changes is primarily due to how the reactivity of weakly nucleophilic Ser, Thr, and Tyr residues are influenced by small changes in their microenvironment. Previous studies have demonstrated that unlike the more highly nucleophilic residues, His and Lys, the reactivity of Ser, Thr, and Tyr are not dictated primarily by their solvent exposure.[36] Instead, a partially exposed hydrophobic microenvironment increases the reactivity of these weakly nucleophilic residues by increasing the local concentration of hydrophobic DEPC. If the microenvironment around a Ser, Thr, or Tyr becomes more hydrophilic because of side chain rearrangements or other HOS changes, the reactivity of the residue will decrease, thus leading to a lower extent of labeling even though the residue might have similar solvent exposure. Measurable changes in deuterium uptake in HDX require making or breaking of H-bonds along the backbone to bury or expose amide hydrogens. Such changes require more energy than simple side chain reorientations, explaining why no HDX changes are observed upon heating at only 45 °C. Together the HDX/MS and CL/MS data suggest structural changes at 45 °C are likely a result of some side chain orientation changes and not large-scale structural or dynamic changes. None of the structural changes is sufficient to cause any measurable change in rituximab activity (Figure S2) or circular dichroism signal (Figure S3).

The DEPC CL/MS and HDX/MS data after heating at 55 °C further demonstrate the greater sensitivity of DEPC CL/MS to rituximab structural changes. Only one peptide has increased exchange in HDX, while CL changes are clustered in the antigen-binding region of the protein and scattered in the F_c region. The CL/MS, and not the HDX/MS data, is consistent with the Raji cell pull-down activity assay at 55 °C (Figure S2C), which indicates a significant change in the F_{ab} region. Two other F_c-specific activity assays, the rituximab bridging ELISA and the Alamar blue assays, are somewhat ambiguous in whether significant changes are occurring in the F_c region. A small, but statistically significant change is detected in F_c binding from the bridging ELISA assay near 55 °C (Figure S2A), but the Alamar blue assay shows no significant change in the activity of the F_c region (Figure S2B). This discrepancy may reflect the scattered changes in labeling extent in the CL/MS data from F_c region. The increase in HDX at 55 °C is not reflected in the activity assays, as no significant changes in deuterium uptake are measured in the antigen-binding or F_c regions. This observation indicates that HDX is not sensitive to the structural changes that influence activity, in the same way CL/MS is. It may be that most of the changes detected by

HDX/MS are changes in backbone dynamics that have little effect on the activity assays. The idea that HDX/MS is reporting on backbone dynamics is further supported by the fact that changes in deuterium uptake upon heating at 55 °C are no longer apparent after 24 h of exchange. After 24 h of exchange, regions that are less dynamic under native conditions can exchange fully, adding deuterium to the same extent as a region made more dynamic upon heating. The different responses of the two MS-based methods can perhaps be understood by appreciating that DEPC-based CL/MS is better at reporting on changes in side chain orientations, interactions, and solvent accessibility, whereas HDX/MS better measures backbone dynamics and backbone solvent accessibility. Since binding in the F_{ab} region, as reported by the activity assays, is mostly mediated by side chain interactions, it is perhaps not surprising that DEPC-CL more sensitively detects these sorts of changes.

Methods are complementary

HDX/MS and CL/MS are complementary methods because HDX provides information about the backbone and CL monitors side chains. The full scope of the methods' complementarity is especially apparent in the 65 °C heat-stress data. Overall, the structural information obtained from both methods is consistent, in that increases take place only in the F_{ab}, while decreases take place throughout the protein, yet each method fills in gaps of information for the other. For example, locations where HDX/MS cannot detect changes, but CL/MS can, is a good demonstration of complementarity. Upon heating at 65 °C, the V_H domain undergoes no significant changes in HDX, but there are six residues (His35, Lys67, Lys74, Ser77, Thr118, and Ser120) that undergo significant changes in CL. The Raji cell pull-down assay shows substantial changes in F_{ab} binding upon heating at 65 °C heat stress, which is consistent with the changes in CL in the V_H domain. The lack of changes in the HDX/MS data in this region might indicate that changes in activity assay are entirely the result of side chain re-orientations and not significant backbone changes in this domain, which would undoubtedly lead to HDX changes. These data illustrate the advantage of using both methods to detect HOS changes. Clearly, if only HDX/MS had been used, structural changes in V_H domain would not have been detected, even though they are substantial enough to affect the activity of rituximab.

Locations where one method indicates an increase in labeling or exchange, while the other indicates a decrease in labeling or exchange could seem contradictory. However, these particular data demonstrate the complementarity of CL/MS and HDX/MS. Our data contain one example of apparently contradictory HDX-MS and CL-MS results. In the V_L domain (Figure 4), there is a peptide that increases (94-103) in HDX, one that decreases (10-24) in HDX, and three residues that decrease in CL (Ser5, Tyr70, and Thr101). The apparent contradiction involves Thr101, which undergoes a CL decrease, while the relatively short peptide that spans this residue undergoes an increase in HDX. It is likely that the V_L domain partially unfolds at 65 °C, leading to an increase in solvent exposure at peptide 94-103 and a decrease in solvent exposure around peptide 10-24 that is caused by aggregation or repacking of the hydrophobic core. The HDX data reveal that residues 10-24 are in a region of conformational heterogeneity as there are two exchange distributions. The decreased deuterium uptake after heating is only observed in the slow-exchanging conformation of the peptide, while the fast-exchanging conformation shows no difference in the stressed and

native states (Figure S10). The differences in deuterium uptake for the peptide 10-24 persists even after 24 h of exchange, suggesting the HOS changes that take place might not be caused by changes in protein dynamics. The increase in solvent exposure at peptide 94-103 likely eliminates hydrophobic contacts with Thr101, creating a more hydrophilic microenvironment that decreases the CL of this residue.[36] Structural changes that affect the microenvironment around Thr101 likely affect the positioning of residues Tyr70 and Ser5 as well. These residues undergo significant decreases in CL and are directly adjacent in 3D space to peptide 10-24, which also decreases in deuterium uptake (Figure 4). The decreases in both methods could be a result of a repacking of the hydrophobic core involving residues Leu11 and Ile10. By interpreting the complex changes detected in the V_L domain by each method, we conclude that significant structural changes are taking place here upon heat stress. Data from both methods thus provide complementary information that yield a more complete picture.

Methods are synergistic

When used together CL/MS can clarify ambiguous HDX/MS data, providing new information that neither method can provide alone. This synergism is a result of the differences in intrinsic reactions rates of each method. The intrinsic or chemical exchange rate of HDX is on the order of ms, which means HDX is sensitive to protein dynamic changes. In contrast, the intrinsic reaction rate of DEPC-CL is on the order of s to min and is not used in a time course, making DEPC-CL essentially blind to protein dynamics.[29] Because of the differences in intrinsic reaction rates, DEPC-CL can clarify ambiguous HDX data, thus providing insight not accessible from HDX-MS. HDX/MS data can sometimes be ambiguous because decreases in exchange can be the result of changes in dynamics or solvent accessibility. DEPC-CL/MS can be used to help determine which of these changes is taking place.

After heating at 65 °C, HDX decreases are measured throughout protein (Figure 3), yet few regions show overlapping decreases in both CL and HDX. As previously discussed, many of the labeling and exchange results provide complementary information (e.g. V_H domain data), so positive correlations for the two methods yield additional information. One such region is the C_{H3} domain in which the peptide 428-450 undergoes significant HDX changes, and several residues in or near this region also undergo decreased CL. As indicated in the Results section, the protein region spanned by residues 428-450 exists in two conformations, with the slow-exchanging conformation decreasing in deuterium uptake after heating and the fast-exchanging conformation increasing in uptake after heating (Figure S12). The decreased exchange in the slow-exchanging conformation together with the decrease in CL in this protein region and sample cloudiness upon heating at 65 °C suggests that protein aggregation is occurring in this domain. The conformational heterogeneity revealed by the HDX data indicates additional unique behavior for this protein region. The increased exchange of the fast-exchanging conformation suggest that some protein molecules unfold in the F_c region instead of aggregate.

In the absence of other experimental data to confirm protein aggregation in the F_c region, we used several aggregation prediction algorithms to identify possible aggregation “hot spots”

in rituximab. Aggregation hotspots that are identified by the algorithms PASTA, AGGRESCAN, and TANGO include regions of the C_{H2} domain, the C_L domain, and the C_{H3} domain (Figure S7),[38-42] Our experimental results are only somewhat consistent with these theoretical predictions. The C_{H2} region is predicted to have the highest likelihood of aggregation, yet we only observe one peptide (268-281) that decreases in HDX and one residue (Ser302) that decreases in CL in this domain upon heating at 65 °C. A larger cluster of HDX/MS and CL/MS decreases would be expected if the C_{H2} domain were an aggregation site. It should be noted that PASTA and TANGO, which most definitively predict aggregation in the C_{H2} domain, are algorithms primarily used to predict amyloid-like aggregation. Thus, these algorithms may not be well suited for predicting mAb aggregation upon heating. Our HDX/MS and CL/MS data do not support the predicted aggregation in the C_L domain. The region in the C_L domain that is predicted to aggregate by AGGRESCAN and TANGO undergoes an increase in HDX upon heating at both the 55 and 65 °C (i.e. peptide 148-171). Moreover, The C_L domain contains 18 labeled residues; however, only one has a significant change in labeling, and it is an increase in labeling (His196).

AGGRESCAN and TANGO also indicate that there are aggregation “hot spots” in the C_{H3} domain. There is a cluster of residues in this domain that undergo decreased CL (Ser428, His439, Tyr440, Lys451) within a region that also undergoes decreased HDX (428-450), suggesting aggregation does occur at this site. HDX/MS data by itself might suggest the C_{H3} region as an aggregation site, but it would also indicate the C_{H2} domain as an aggregation site because the residues 268-281 in this domain undergo a significant decrease in exchange as well. However, there are three DEPC labelable residues in the span from 268 to 281, and none of them undergo a significant decrease in CL upon heating. Based on the reaction timescales of the two methods, a decrease in HDX that does not coincide with a decrease in CL suggests reduced backbone dynamics, rather than a site of aggregation. Drawing this conclusion from the HDX/MS data alone would be difficult, although using much longer exchange times (≥ 24 h) can sometimes distinguish between decreased protein dynamics and aggregation. However, if the aggregated protein molecules are in equilibrium with un-aggregated protein molecules, as the multiple exchange distributions observed in the HDX data suggest, even longer exchange times might not accurately distinguish between aggregated sites and decreased protein dynamics. Additionally, it is possible that soluble aggregates become insoluble at longer times, rendering them undetectable by HDX at longer exchange times (>24 h). When considered together, the HDX/MS and CL/MS data indicate that predicted aggregation in the C_{H2} and C_L domains is not observed experimentally, but the predicted aggregation in the C_{H3} domain is. Overall, the differences in intrinsic reaction rates of HDX and CL allow us to obtain clearer information about the structural and dynamic changes caused by heat stress to rituximab.

Conclusions

We have demonstrated here that HDX and DEPC-CL provide complementary, and sometimes synergistic, information about structural perturbations undergone by mAbs upon exposure to heat stress. We find that DEPC-CL uniquely detects subtle shifts in side chain orientation, as demonstrated by heating rituximab at 45 °C for 4 h. Upon this mild heating, changes in DEPC-CL/MS were detected throughout the protein, while no significant

changes in HDX were measured. Under higher heat-stress conditions, results from the two methods complement one another. CL/MS can reveal changes in side chain orientation and solvent exposure that are not accompanied by changes in backbone solvent exposure or dynamics. On the other hand, HDX/MS is sensitive to changes in backbone dynamics that are not accompanied by changes in side chain orientation or solvent exposure. This capability is exemplified by changes that are observed in the V_L domain upon heating at 65 °C. Finally, under conditions that lead to aggregation, the two techniques work synergistically to identify likely aggregation sites. This synergy is a result of differences in the intrinsic reactions rates. The intrinsic reaction rate of HDX is fast enough for HDX/MS to report on changes in protein dynamics, while the slower intrinsic reaction rate of DEPC-CL and the way we apply it means this method is blind to changes in dynamics. Due to differences in their intrinsic reactions rates, DEPC-CL can be used to clarify ambiguous HDX/MS data, as demonstrated by changes in labeling and exchange in the C_{H3} and C_{H2} domain upon heating at 65 °C. Both domains contain peptides that undergo decreased HDX after heat stress, but only the C_{H3} domain also undergoes decreased DEPC CL, indicating this region as a likely aggregation site. Given the complementarity of the two methods, HDX/MS and CL/MS together should be amenable for studies of the HOS perturbations of other protein therapeutics. Moreover, these methods should be applicable to epitope and paratope mapping studies and biosimilar evaluation, while providing deeper structural insight that could improve protein therapeutic design.

Supplementary Material

Refer to Web version on PubMed Central for supplementary material.

Acknowledgements

The authors wish to thank the Institute of Applied Life Sciences mass spectrometry center and Prof. Stephen J. Eyles for his help with the operation of the Thermo Scientific Orbitrap Fusion mass spectrometer. The authors also thank Eric Graban and Dr. John Hale from QuarryBio for access to their custom software pipeline for analyzing the CL/MS data.

Funding

This work was partially supported by the National Institutes of Health (NIH) for Small Business Innovation Research (SBIR) under grant R43 GM116211 and partially supported by NIH grant R01 GM075092. Acquisition of the Thermo Scientific Orbitrap Fusion was made possible by NIH grant S10OD010645. The content is solely the responsibility of the authors and does not necessarily represent the official views of NIH.

References

(1). Lu R; Hwang Y; Liu T; Lee C; Tsai H; Li H; Wu H Development of Therapeutic Antibodies for the Treatment of Diseases. J. Biomed. Sci 2020, 27 (1), 1–30. [PubMed: 31894001]

(2). Ecker DM; Jones SD; Levine HL The Therapeutic Monoclonal Antibody Market. MAbs 2015, 7 (1), 9–14. [PubMed: 25529996]

(3). Nelson AL; Dhimolea E; Reichert JM Development Trends for Human Monoclonal Antibody Therapeutics. Nat. Rev. Drug Discov 2010, 9, 767–774. 10.1038/nrd3229. [PubMed: 20811384]

(4). Elgundi Z; Reslan M; Cruz E; Sifniotis V; Kayser V The State-of-Play and Future of Antibody Therapeutics. Adv. Drug Deliv. Rev 2017, 122, 2–19. 10.1016/j.addr.2016.11.004. [PubMed: 27916504]

(5). Frokjaer S; Otzen D Protein Drug Stability: A Formulation Challenge. Nat. Rev. Drug Discov 2005, 4 (5), 298–306. 10.1038/nrd1695. [PubMed: 15803194]

(6). Berkowitz SA; Engen JR; Mazzeo JR; Jones GB Analytical Tools for Characterizing Biopharmaceuticals and the Implications for Biosimilars. Nat. Rev. Drug Discov 2012, 11, 527–540. 10.1038/nrd3746. [PubMed: 22743980]

(7). Rogstad S; Faustino A; Ruth A; Keire D; Boyne M; Park J Retrospective Evaluation of the Use of Mass Spectrometry in FDA Biologics License Applications. Am. Soc. Mass Spectrom 2017, 28, 786–794. 10.1007/s13361-016-1531-9.

(8). Beck A; Sanglier-Cianéerani S; Van Dorsselaer A Biosimilar, Biobetter, and Next Generation Antibody Characterization by Mass Spectrometry. Anal. Chem 2012, 84 (11), 4637–4646. 10.1021/ac3002885. [PubMed: 22510259]

(9). Artigues A; Nadeau OW; Rimmer MA; Villar MT; Du X; Fenton AW; Carlson GM Protein Structural Analysis via Mass Spectrometry-Based Proteomics. Adv. Exp. Med. Biol 2016, 919, 397–431. 10.1007/978-3-319-41448-5. [PubMed: 27975228]

(10). Huang RY; Chen G Higher Order Structure Characterization of Protein Therapeutics by Hydrogen/Deuterium Exchange Mass Spectrometry. Anal Bioanal Chem 2014, 406, 6541–6558. 10.1007/s00216-014-7924-3. [PubMed: 24948090]

(11). Edgeworth MJ; Phillips JJ; Lowe DC; Kippen AD; Higazi DR; Scrivens JH Global and Local Conformation of Human IgG Antibody Variants Rationalizes Loss of Thermodynamic Stability. Angew. Chemie - Int. Ed 2015, 54 (50), 15156–15159. 10.1002/anie.201507223.

(12). Marciano DP; Dharmarajan V; Griffin PR HDX-MS Guided Drug Discovery: Small Molecules and Biopharmaceuticals. Curr. Opin. Struct. Biol 2014, 28, 105–111. 10.1016/j.sbi.2014.08.007. [PubMed: 25179005]

(13). Konermann L; Pan J; Liu Y-H Hydrogen Exchange Mass Spectrometry for Studying Protein Structure and Dynamics. R. Soc. Chem 2011, 1224–1234. 10.1039/c0cs00113a.

(14). Zhang MM; Huang RYC; Beno BR; Deyanova EG; Li J; Chen G; Gross ML Epitope and Paratope Mapping of PD-1/Nivolumab by Mass Spectrometry-Based Hydrogen-Deuterium Exchange, Cross-Linking, and Molecular Docking. Anal. Chem 2020, 92 (13), 9086–9094. 10.1021/acs.analchem.0c01291. [PubMed: 32441507]

(15). Iacob RE; Bou-assaf GM; Makowski LEE; Engen JR; Berkowitz SA; Houde D Investigating Monoclonal Antibody Aggregation Using a Combination of H / DX-MS and Other Biophysical Measurements. J. Pharm. Sci 2013, 102, 4315–4329. 10.1002/jps.23754. [PubMed: 24136070]

(16). Wei H; Mo J; Tao L; Russell RJ; Tymiak AA; Chen G; Iacob RE; Engen JR Hydrogen/Deuterium Exchange Mass Spectrometry for Probing Higher Order Structure of Protein Therapeutics: Methodology and Applications. Drug Discov. Today 2015, 19 (1), 95–102. 10.1016/j.drudis.2013.07.019.Hydrogen/Deuterium.

(17). Huang RYC; Krystek SR; Felix N; Graziano RF; Srinivasan M; Pashine A; Chen G Hydrogen/Deuterium Exchange Mass Spectrometry and Computational Modeling Reveal a Discontinuous Epitope of an Antibody/TL1A Interaction. MAbs 2018, 10 (1), 95–103. 10.1080/19420862.2017.1393595. [PubMed: 29135326]

(18). Pan J; Zhang S; Chou A; Borchers CH Higher-Order Structural Interrogation of Antibodies Using Middle-down Hydrogen/Deuterium Exchange Mass Spectrometry. Chem. Sci 2016, 7(2), 1480–1486. 10.1039/c5sc03420e. [PubMed: 29910905]

(19). Liu T; Marcinko TM; Kiefer PA; Vachet RW Using Covalent Labeling and Mass Spectrometry To Study Protein Binding Sites of Amyloid Inhibiting Molecules. Anal. Chem 2017, 89, 11583–11591. 10.1021/acs.analchem.7b02915. [PubMed: 29028328]

(20). Liu XR; Zhang MM; Gross ML Mass Spectrometry-Based Protein Footprinting for Higher-Order Structure Analysis: Fundamentals and Applications. Chem. Rev 2020, 120, 4355–4454. 10.1021/acs.chemrev.9b00815. [PubMed: 32319757]

(21). Cornwell O; Radford SE; Ashcroft AE; Ault JR Comparing Hydrogen Deuterium Exchange and Fast Photochemical Oxidation of Proteins: A Structural Characterisation of Wild-Type and ΔN6 B2-Microglobulin. J. Am. Soc. Mass Spectrom 2018, 29, 2413–2426. 10.1007/s13361-018-2067-y. [PubMed: 30267362]

(22). Li KS; Shi L; Gross ML Mass Spectrometry-Based Fast Photochemical Oxidation of Proteins (FPOP) for Higher Order Structure Characterization. Acc. Chem. Res 2018, 51, 736–744. 10.1021/acs.accounts.7b00593. [PubMed: 29450991]

(23). Limpikirati P; Liu T; Vachet RW Covalent Labeling-Mass Spectrometry with Non-Specific Reagents for Studying Protein Structure and Interactions. Methods 2018, 144, 79–93. 10.1016/j.ymeth.2018.04.002. [PubMed: 29630925]

(24). Kaur P; Tomechko SE; Kiselar J; Shi W; Deperalta G; Wecksler AT; Gokulrangan G; Ling V; Chance MR Characterizing Monoclonal Antibody Structure by Carboxyl Group Footprinting. MAbs 2015, 7 (3), 540–552. [PubMed: 25933350]

(25). Limpikirati P; Hale JE; Hazelbaker M; Huang Y; Jia Z; Yazdania M; Grabanb EM; Vaughan RC; Vachet RW Covalent Labeling and Mass Spectrometry Reveal Subtle Higher Order Structural Changes for Antibody Therapeutics. MAbs 2019, 11 (3), 463–476. 10.1080/19420862.2019.1565748. [PubMed: 30636503]

(26). Li KS; Chen G; Mo J; Huang RY; Deyanova EG; Beno BR; O'Neil SR; Tymiak AA; Gross ML Orthogonal Mass Spectrometry-Based Footprinting for Epitope Mapping and Structural Characterization: The IL-6 Receptor upon Binding of Protein Therapeutics. Anal. Chem 2017, 89, 7742–7749. 10.1021/acs.analchem.7b01748. [PubMed: 28621526]

(27). Pan Y; Piyadasa H; O'Neil JD; Konermann L Conformational Dynamics of a Membrane Transport Protein Probed by H/D Exchange and Covalent Labeling: The Glycerol Facilitator. J. Mol. Biol 2012, 416 (3), 400–413. 10.1016/j.jmb.2011.12.052. [PubMed: 22227391]

(28). Zheng X; Wintrode PL; Chance MR Complementary Structural Mass Spectrometry Techniques Reveal Local Dynamics in Functionally Important Regions of a Metastable Serpin. Cell Press 2008, 16, 38–51. 10.1016/j.str.2007.10.019.

(29). Liu T; Limpikirati P; Vachet RW Synergistic Structural Information from Covalent Labeling and Hydrogen – Deuterium Exchange Mass Spectrometry for Protein – Ligand Interactions. Anal. Chem 2019, 91, 15248–15254. 10.1021/acs.analchem.9b04257. [PubMed: 31664819]

(30). Limpikirati PK; Zhao B; Pan X; Eyles SJ; Vachet RW Covalent Labeling/Mass Spectrometry of Monoclonal Antibodies with Diethylpyrocarbonate: Reaction Kinetics for Ensuring Protein Structural Integrity. J. Am. Soc. Mass Spectrom 2020, 31 (6), 1223–1232. 10.1021/jasms.0c00067. [PubMed: 32310649]

(31). Borotto NB; Zhou Y; Hollingsworth SR; Hale JE; Graban EM; Vaughan RC; Vachet RW Investigating Therapeutic Protein Structure with Diethylpyrocarbonate Labeling and Mass Spectrometry. Anal. Chem 2015, 87, 10627–10634. 10.1021/acs.analchem.5b03180. [PubMed: 26399599]

(32). Krezel A; Bal W A Formula for Correlating PKa Values Determined in D2O and H2O. J. Inorg. Biochem 2004, 98, 161–166. 10.1016/j.jinorgbio.2003.10.001. [PubMed: 14659645]

(33). Masson GR; Burke JE; Ahn NG; Anand GS; Borchers C; Brier S; Bou-assaf GM; Engen JR; Englander SW; Faber J; Garlish R; Griffin PR; Gross ML; Guttman M; Hamuro Y; Heckle AJR; Houde D; Iacob RE; Jørgensen TJD; Kaltashov IA; Klinman JP; Konermann L; Man P; Mayne L; Pascal BD; Reichmann D; Skehel M; Snijder J; Strutzenberg TS; Underbakke ES; Wagner C; Wales TE; Walters BT; Weis DD; Wilson DJ; Wintrode PL; Zhang Z; Zheng J; Schriemer DC; Rand KD Recommendations for Performing, Interpreting and Reporting Hydrogen Deuterium Exchange Mass Spectrometry (HDX-MS) Experiments. Nat. Methods 2019, 16, 595–602. 10.1038/s41592-019-0459-y. [PubMed: 31249422]

(34). Padlan EA Anatomy of the Antibody Molecule. Mol. Immunol 1994, 31 (3), 169–217. [PubMed: 8114766]

(35). Andersen CB; Manno M; Rischel C; Thorolfsson M; Martorana V Aggregation of a Multidomain Protein : A Coagulation Mechanism Governs Aggregation of a Model IgG1 Antibody under Weak Thermal Stress. Protein Sci. 2010, 19, 279–290. 10.1002/pro.309. [PubMed: 20014440]

(36). Limpikirati P; Pan X; Vachet RW Covalent Labeling with Diethylpyrocarbonate: Sensitive to the Residue Microenvironment, Providing Improved Analysis of Protein Higher Order Structure by Mass Spectrometry. Anal. Chem 2019, 91 (13), 8516–8523. 10.1021/acs.analchem.9b01732. [PubMed: 31150223]

(37). Li J; Wei H; Krystek SR; Bond D; Brender TM; Cohen D; Feiner J; Hamacher N; Harshman J; Huang RY; Julien SH; Lin Z; Moore K; Mueller L; Noriega C; Sejwal P; Sheppard P; Stevens B;

Chen G; Tymiak AA; Gross ML; Schneeweis LA Mapping the Energetic Epitope of an Antibody/Interleukin-23 Interaction with Hydrogen/Deuterium Exchange, Fast Photochemical Oxidation of Proteins Mass Spectrometry, and Alanine Shave Mutagenesis. Anal. Chem 2017. 10.1021/acs.analchem.6b03058.

(38). Linding R; Schymkowitz J; Rousseau F; Diella F; Serrano L A Comparative Study of the Relationship between Protein Structure and β-Aggregation in Globular and Intrinsically Disordered Proteins. J. Mol. Biol 2004, 342 (1), 345–353. 10.1016/j.jmb.2004.06.088. [PubMed: 15313629]

(39). Van Der Kant R; Karow-zwick AR; Van Durme J; Blech M; Gallardo R; Seeliger D; Aßfalg K; Baatsen P; Compernolle G; Gils A; Studts JM; Schulz P; Garidel P; Schymkowitz J; Rousseau F Prediction and Reduction of the Aggregation of Monoclonal Antibodies. J. Mol. Biol 2017, 429 (8), 1244–1261. 10.1016/j.jmb.2017.03.014. [PubMed: 28322916]

(40). Fernandez-Escamilla AM; Rousseau F; Schymkowitz J; Serrano L Prediction of Sequence-Dependent and Mutational Effects on the Aggregation of Peptides and Proteins. Nat. Biotechnol 2004, 22 (10), 1302–1306. 10.1038/nbt1012. [PubMed: 15361882]

(41). Conchillo-Solé O; de Groot NS; Avilés FX; Vendrell J; Daura X; Ventura S AGGRESCAN: A Server for the Prediction and Evaluation of “Hot Spots” of Aggregation in Polypeptides. BMC Bioinformatics 2007, 8. 10.1186/1471-2105-8-65.

(42). Walsh I; Seno F; Tosatto SCE; Trovato A PASTA 2.0: An Improved Server for Protein Aggregation Prediction. Nucleic Acids Res. 2014, 42, 301–307. 10.1093/nar/gku399.

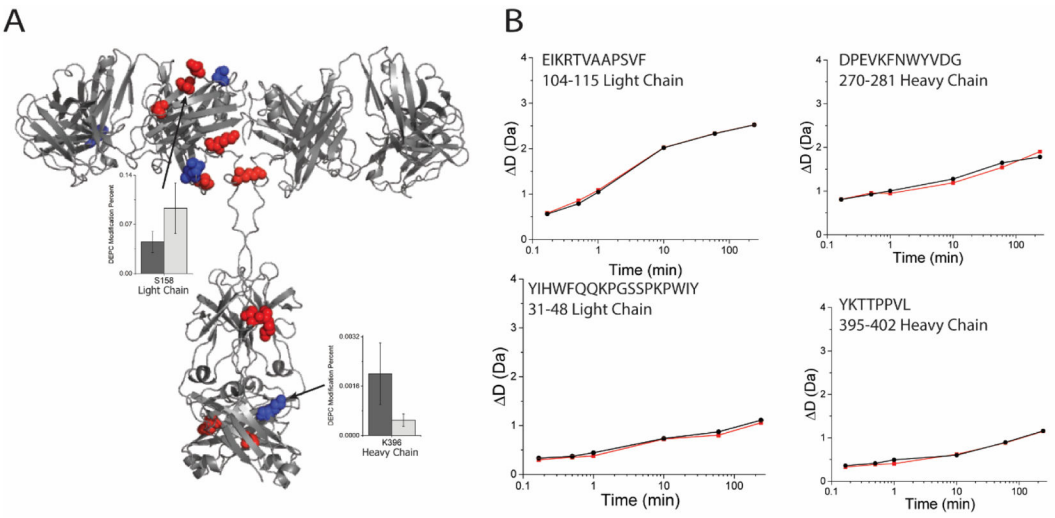

Figure 1:

DEPC CL/MS and HDX/MS results of heat stressed (4 h at 45 °C) rituximab. (A) DEPC CL changes. Residues depicted in red represent increases in CL extent while residues in blue represent decreases in CL extent. Representative plots of change in labeling extent are shown for residues Ser158 and Lys396. Dark gray indicates the native state while the light gray indicates the heat stressed state. Changes are scattered throughout the entire protein with no clustering, which indicates a lack of substantial HOS changes. Atomic coordinates of an existing IgG1 F_{ab} crystal structure (PDB 1FC2) and a generic IgG1 F_c crystal structure (PDB 2IG2) were used as templates to generate the rituximab structure, with the hinge region theoretically modeled.[34] The F_c (PDB 4W4N) and F_{ab} (PDB 4KAQ) structures of rituximab were then aligned to the template, using the molecular visualization system PyMOL. For clarity, CL on only one light chain and one heavy chain are indicated. (B) Representative deuterium uptake plots from HDX/MS of rituximab after heating at 45 °C. The unheated state is shown in black, and the heat-stressed state is shown in red. No measurable difference in deuterium uptake is observed.

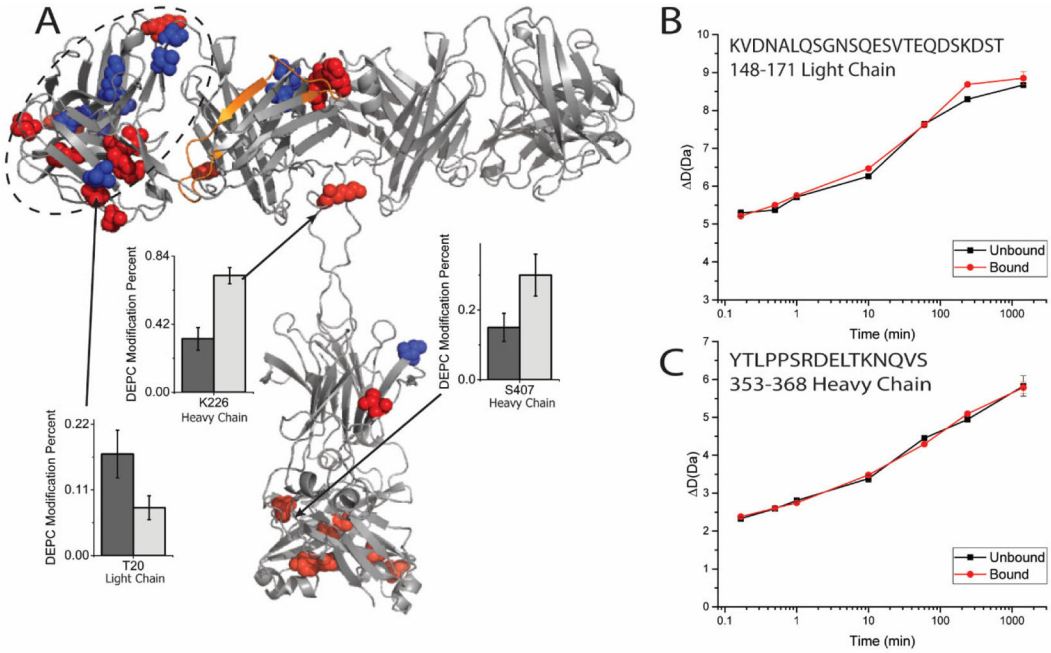

Figure 2:

DEPC CL/MS and HDX/MS of heat stressed (4 h at 55 °C) rituximab. (A) DEPC CL and HDX changes. Residues depicted in red represent increases in CL extent while residues in blue represent decreases in CL extent. Residues that undergo changes in CL extent are clustered in the F_{ab} (circled with a dotted black line). Representative plots of CL/MS changes in labeling extent are shown for residues Lys226, Thr20, and Ser407. Dark gray indicates the native state while the light gray indicates the heat stressed state. Highlighted in orange on the structure is the peptide that undergoes increased HDX. Details of the molecular model of rituximab are found in the Figure 1 caption. For clarity, only labeling on one heavy chain and one light chain is shown. (B) Deuterium uptake plot from HDX/MS of rituximab after heating at 55 °C for peptide 148-171 that experiences a significant change in uptake. The unheated state is in black, and the heat-stressed state is shown in red. (C) Representative deuterium uptake plot from HDX/MS of rituximab after heating at 55 °C for peptide 353-368 that does not experience a significant change in uptake. The unheated state is in black, and the heat-stressed state is shown in red. Peptides were found to be statistically different if they were 3σ outside of the average of all differences for all time points and for all peptides.

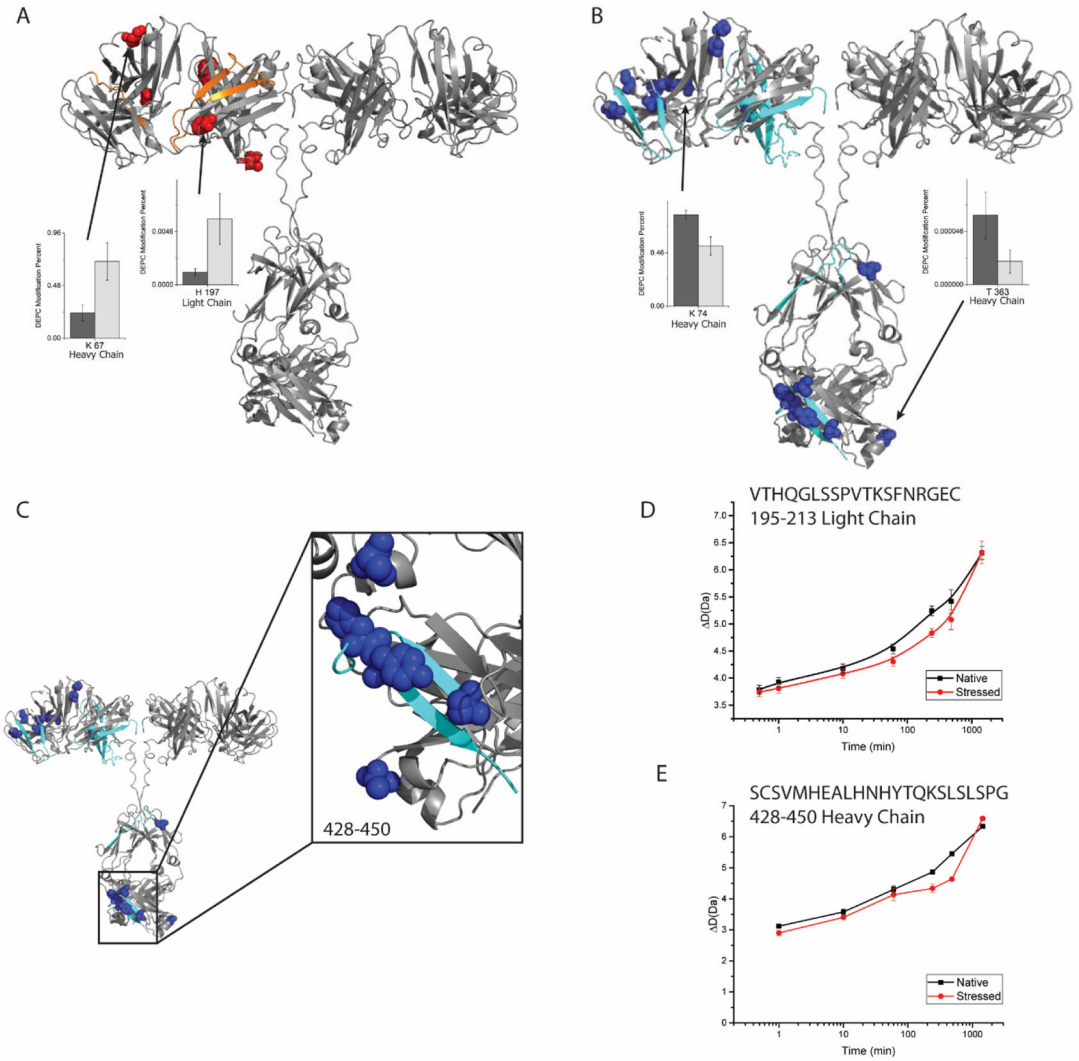

Figure 3:

DEPC CL/MS and HDX/MS of heat stressed (4 h at 65 °C) rituximab. (A) Increases in DEPC CL extent and HDX uptake. Residues depicted in red represent increases in CL extent while peptides highlighted in orange represent increases in deuterium uptake. Representative plots of change in labeling extent are shown for residues Lys67 and His197. Dark gray indicates the native state while the light gray indicates the heat stressed state. (B) DEPC CL/MS and HDX/MS decreases. Residues depicted in blue represent increases in CL extent while peptides highlighted in cyan represent increases in deuterium uptake. Representative plots of change in labeling extent are shown for residues Lys74 and Thr363. Dark gray indicates the native state while the light gray indicates the heat stressed state. (C) Expanded view of the C_{H3} region where decreases overlap from both methods. (D, E) Representative deuterium uptake plots from HDX/MS of rituximab after heating at 65 °C. The unheated state is shown in black, and the heat-stressed state is shown in red. Peptides were found to be statistically different if they were 3σ outside of the average of all differences for all time points and for all peptides.

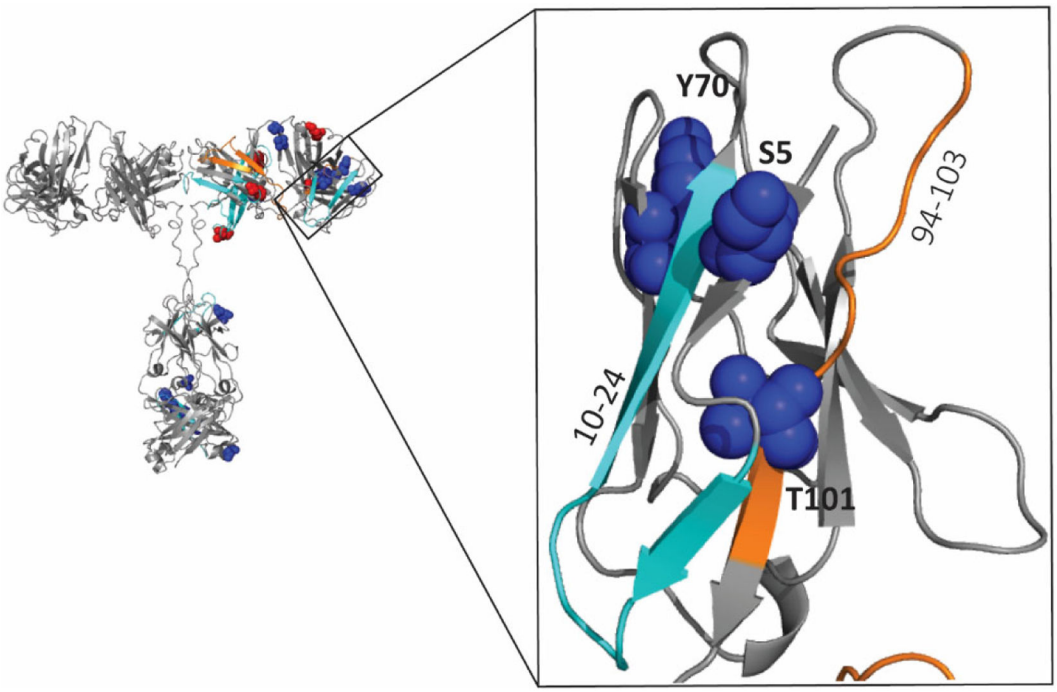

Figure 4:

Expanded view of the V_L domain of rituximab and the CL/MS and HDX/MS changes that occur in this region upon heat stress at 65 °C for 4 h. Residues indicated in blue spheres undergo decreased CL upon heating. The strands in orange and cyan represent peptides that undergo increased or decreased HDX, respectively, upon heating. The peptide 10-24 becomes more solvent exposed, eliminating the hydrophobic microenvironment around Thr101, while peptide 94-103 experiences a decrease in solvent exposure as a result of aggregation or repacking of the hydrophobic core.

Table 1:

Table of significant changes in DEPC labeling extent under different heat-stress conditions

Residue	Native	Stressed
45 °C for 4 h		
Light chain		
Ser155	5 ± 2%	9 ± 4%
Ser158	5 ± 2%	9 ± 4%
Ser161	5 ± 2%	9 ± 4%
Ser181	1.0 ± 0.5%	0.31 ± 0.06%
Heavy chain		
Ser76	26 ± 7%	6 ± 4%
Ser77	14 ± 4%	2 ± 2%
Lys137	0.05 ± 0.02%	0.2 ± 0.1%
Ser140	0.3 ± 0.2%	0.06 ± 0.03%
Thr143	0.3 ± 0.2%	0.07 ± 0.04%
Ser194	0.04 ± 0.02%	0.2 ± 0.1%
Lys226	40 ± 10%	73 ± 20%
Thr293	7 ± 3%	20 ± 10%
Lys294	7 ± 3%	20 ± 10%
Thr370	8 ± 1%	14 ± 4%
Lys374	8 ± 1%	14 ± 4%
Lys396	0.2 ± 0.1%	0.05 ± 0.02%
Ser448	17 ± 2%	26 ± 4%
55 °C for 4		
Residue	**Native**	**Stressed**
Light chain		
Thr20	17 ± 4%	8 ± 2%
His33	0.08 ± 0.02%	0.20 ± 0.02%
Lys44	0.06 ± 0.02%	0.15 ± 0.01%
Thr73	50 ± 10%	86 ± 3%
Ser75	50 ± 10%	86 ± 3%
Thr84	1.3 ± 0.2%	2.6 ± 0.5%
Tyr85	1.3 ± 0.2%	2.6 ± 0.5%
Thr91	0.03 ± 0.02%	0.10 ± 0.01%
Thr128	5 ± 1%	3.1 ± 0.3%
Ser130	5 ± 1%	3.1 ± 0.3%
Tyr185	23.5 ± 0.3%	27 ± 2%
His188	55 ± 2%	64 ± 3%
Heavy Chain		
Lys13	2.7 ± 0.5%	3.7 ± 0.3%

Residue	Native	Stressed
Ser21	24 ± 4%	11 ± 4%
His35	23 ± 3%	4 ± 1%
Lys38	30 ± 2%	22 ± 3%
Lys74	79 ± 4%	87 ± 1%
Ser76	2.4 ± 0.2%	1.5 ± 0.2%
Thr118	71 ± 3%	59 ± 7%
Ser120	84 ± 2%	70 ± 7%
Ser164	0.002 ± 0.001%	0.016 ± 0.005%
Lys226	33 ± 7%	72 ± 5%
Thr293	38 ± 6%	85 ± 8%
Ser302	38 ± 3%	16 ± 6%
Tyr353	0.4 ± 0.6%	14 ± 2%
Thr363	0.006 ± 0.002%	0.012 ± 0.003%
Ser368	0.02 ± 0.02%	0.18 ± 0.01%
Ser407	15 ± 4%	30 ± 6%
Tyr411	7 ± 5%	20 ± 4%
Ser448	70 ± 10%	92 ± 4%
Lys451	40 ± 30%	79 ± 7%
65 °C for 4 h		
Residue	**Native**	**Stressed**
Light chain		
Ser5	0.03 ± 0.01%	0.01 ± 0.01%
Tyr70	14 ± 5%	2 ± 2 %
Thr101	0.18 ± 0.01%	0.07 ± 0.05%
His197	0.11 ± 0.03%	0.6 ± 0.2%
Heavy Chain		
His35	23 ± 3%	11 ± 3%
Lys67	23 ± 7%	70 ± 20%
Lys74	79 ± 4%	52 ± 8%
Ser77	0.01 ± 0.01%	0.03 ± 0.01%
Thr118	71 ± 3%	55 ± 5%
Ser120	84 ± 2%	69 ± 4%
Ser161	1.8 ± 0.2%	1.2 ± 0.2%
Ser196	0.01 ± 0.00%	0.08 ± 0.02%
Thr199	0.01 ± 0.00%	0.05 ± 0.02%
His208	0 ± 0%	0.04 ± 0.01%
Ser211	0 ± 0%	0.21 ± 0.02%
Ser258	5 ± 2%	1 ± 1%
Ser302	38 ± 3%	10 ± 10%

Residue	Native	Stressed
Thr363	0.006 ± 0.002%	0.002 ± 0.001%
Ser428	0.86 ± 0.08%	0.4 ± 0.2%
His439	5.4 ± 0.9%	2.5 ± 0.3%
Tyr440	0.02 ± 0.01%	0.01 ± 0.01%
Lys451	40 ± 20%	5 ± 5%

Table 2:

Comparison of HDX and CL changes

Covalently labeled residues that fall within peptides that have:	Sites of CL Increases		Sites of CL Decreases	
	Light Chain	Heavy Chain	Light Chain	Heavy Chain
No Change in HDX	His197	Lys 67, Ser196, Thr199, His208	Ser5, Tyr70,	His35, Lys74, Thr118, Ser120, Ser161, Ser258, Ser302, Thr363
Opposite change as HDX	None		Thr101	None
Same change as HDX	None		None	Ser428, His439, Tyr440, Lys451
No HDX coverage	None	Ser77, Ser211	None	